Modified Gain and Mode Characteristics in Two-Dimensional Photonic Crystal Waveguide With Microcavity Structure

Kaiyu Cui, Yidong Huang, *Member, IEEE*, Wei Zhang, and Jiangde Peng

***Abstract*—Optical gain spectra of InGaAsP MQW for photonic crystal waveguide (PCWG) were simulated by the $k \cdot p$ method with considering the variation of group velocity and the natural broadening synthetically. The dependence of the first mode's gain maximum on the width of PCWG was discussed. To improve the mode characteristics and the gain performances in the 2-D PCWG with relative large width, we proposed a new structure by combining a microcavity inside the 2-D PCWG. Mode characteristics in proposed structure were analyzed and the transmission performance was simulated by the FDTD method. The simulation results show that improved longitudinal mode characteristics can be obtained even in the W3 PCWG with relative wide waveguide width because of the additional frequency selecting mechanism provided by the microcavity.**

***Index Terms*—Microcavity, optical gain, photonic crystal, waveguide.**

I. Introduction

TWO-DIMENSIONAL photonic crystal waveguide (2-D PCWG) has attracted a lot of attention because of its potential applications on photonic integrated circuits as passive and active devices [1], [2]. The typical 2-D PCWG structures are W1 and W3 PCWG, which are formed by taking one or three rows away from the triangular lattice of photonic crystal [3]. Since Dowling [4] first pointed out that the remarkable gain enhancement near the photonic band edge, a lot of studies have been done theoretically and experimentally [5]–[8]. However, how to deal with the gain singularities caused by the abnormal group velocity at the band edge is still an important pending issue, and mode characteristics of 2-D PCWG, which determines the gain characteristics of the PCWG, also need to be further investigated. It is known that W1 PCWG, which has relatively good mode characteristics, is too narrow to be fabricated and especially hard to realize electrical injection structure for some active devices (only about $\sqrt{3}a - 2r \approx 0.4$ μm waveguide width without holes for 1.55-μm wavelength, a and r denote period and radius of holes in PCWG, respectively). Compared to W1 PCWG, W3 PCWG has larger width (about $2\sqrt{3}a - 2r \approx 1.2$ μm waveguide width without holes for 1.55–μm wavelength). Unfortunately, more defect modes appear in W3 PCWG's photonic band gap (PBG), as well as a mini stop-band (MSB) caused by the energy coupling from the fundamental mode to the higher mode [9]. The complex defect modes in W3 PCWG will degrade not only their transmission performance, but also the gain characteristics. In this paper, the optical gain spectra of W1 and W3 PCWG were simulated by the $k \cdot p$ method considering the variation of group velocity and the natural broadening synthetically near the band edge, and the dependence of gain maximum on the width of PCWG was discussed. Based on it, a 2-D PCWG with a microcavity structure is proposed. Simulation results show that improved mode characteristics can be obtained, even in the W3 PCWG with relative wide waveguide width because of the additional frequency selecting mechanism provided by the microcavity.

Manuscript received September 9, 2007; revised February 5, 2008. This work was supported in part by the National Natural Science Foundation of China (NSFC-60537010) and in part by the National Basic Research Program of China (973 Program) under Contract 2007CB307004 and Contract 2006CB302804.

The authors are with the Department of Electronic Engineering, Tsinghua University, Beijing, 100084, China (e-mail: cuiky05@mails.tsinghua.edu.cn; yidonghuang@mail.tsinghua.edu.cn; zwei@mail.tsinghua.edu.cn; pengjd@mail.tsinghua.edu.cn).

Color versions of one or more of the figures in this paper are available online at http://ieeexplore.ieee.org.

Digital Object Identifier 10.1109/JLT.2008.923634

II. Theory and Results

A. Optical Gain Characteristics in 2-D PCWG

The gain simulation in 2-D PCWG was based on the calculation of photonic energy band and the $k \cdot p$ method which is derived from the Fermi's golden rule [10]. To take into account of the valence subband mixture, the 4×4 Luttinger–Kohn Hamiltonian was considered [11]. Because the lifetime of a given state (τ_{in}) in not infinite, the time dependent state has a Lorentzian lineshape $L(\omega)$ in the Fourier energy spectrum. Hence, the energy of each state and each transition has an energy spread over a range of $\Delta E \approx \hbar/\tau_{\mathrm{in}}$, which is the natural broadening of the semiconductor's intraband relaxation process. This means that an incoming photon with energy $\hbar\omega$ will interact with an energy spread of $E \approx \hbar\omega \pm \Delta E$ [10]. Therefore, synthesizing the effect that the gain is in inverse proportion to the changed group velocity v_{g} [4], the optical gain of PCWG can be calculated by the following functions:

$$G(\hbar\omega_{\mathrm{k}}) = \int \alpha(\omega) g(\hbar\omega_{\mathrm{k}}) L(\omega) d\omega \tag{1}$$

$$\alpha(\omega) = \frac{1}{v_{\mathrm{g}}} \bigg/ \frac{1}{v_0} \tag{2}$$

$$L(\omega) = \frac{1/\tau_{\mathrm{in}}}{(\omega - \omega_{\mathrm{k}})^2 + (1/\tau_{\mathrm{in}})^2} \tag{3}$$

where $\alpha(\omega)$ is the gain enhancement factor, which is caused by the low v_{g} of PCWG. v_0 is group velocity of a normal WG.

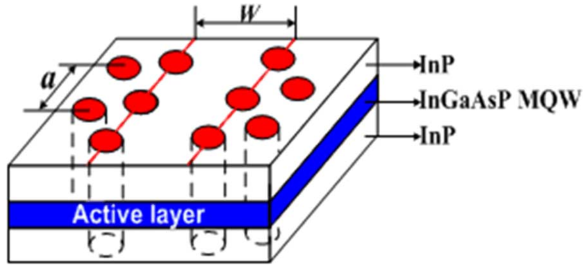

Fig. 1. Simulation model of different PCWG with a line defect waveguide along ΓK direction. The PCWG is fabricated in an InP/InGaAsP/InP heterostructure, containing a layer of MQW with 1.55-μm emission wavelength. The period a for different PCWG were fixed to make their first defect mode's centre correspond to 1.55 μm. The air filling factor is 33% and the holes are etched deep into the InP substrate. The pumped area is focused on the waveguides of PCWG.

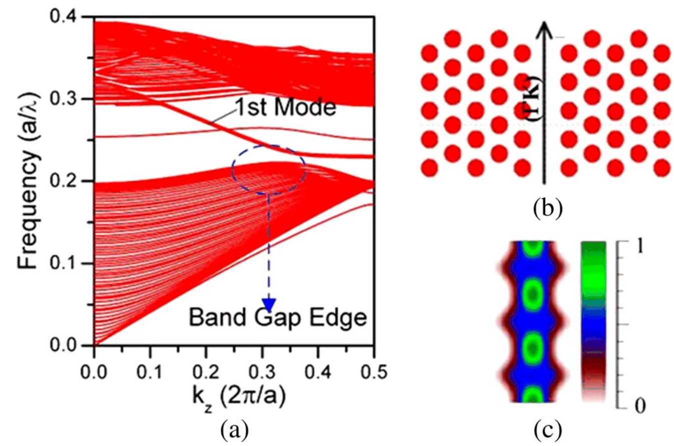

Fig. 2. Photonic energy band structure of W1 PCWG was plotted in (a). The first mode is the fundamental defect mode of the PCWG. (b) W1 PCWG structure along ΓK-direction. (c) Magnetic field pattern of the first mode in W1 PCWG.

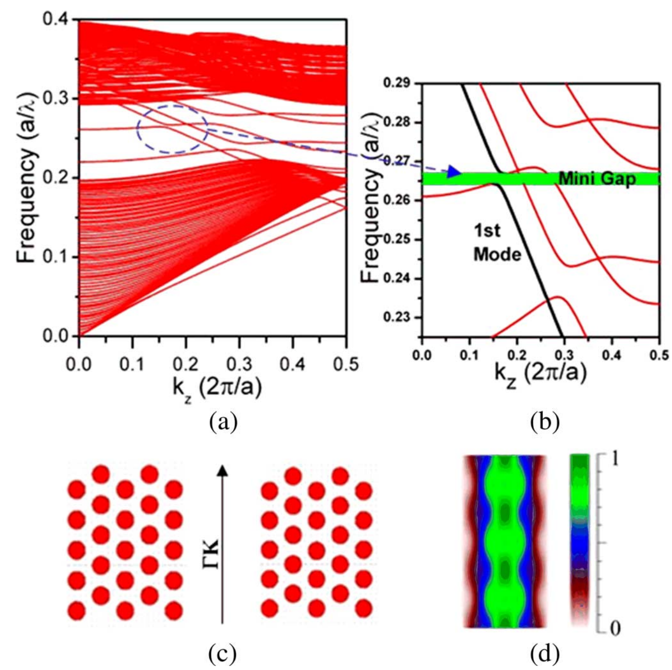

Fig. 3. Photonic energy band structure of W3 PCWG was plotted in (a). Graph (b) is the magnified image for the MSB of the first mode in W3 PCWG. (c) W3 PCWG structure along ΓK-direction. (d) Magnetic field pattern of the first mode in W3.

$L(\omega)$ is a normalized Lorentzian lineshape broadening function, and $g(\hbar\omega_{\rm k})$ is the gain contribution of the transition energy $\hbar\omega$ to $\hbar\omega_{\rm k}$, which is caused by the natural broadening process. The intraband relaxation time (just the lifetime of a given state) $\tau_{\rm in}$ used in our simulation is 10^{-13} s [13]. It is known that the natural broadening, which exists in each transition between the electrons and the holes, should be considered in the semiconductor gain spectra calculation, no matter with or without PC structures [7], [10]. Because the gain is inverse proportion to the changed group velocity $v_{\rm g}$ [4], omitting the natural broadening in PC structures will not only result in errors in the calculation results, but also makes it difficult to deal with the gain spectra at the photonic band edge where the group velocity $v_{\rm g}$ turns to be zero. Natural broadening can mitigate the gain singularities caused by $v_{\rm g}$ turning to be zero near the band edge. Here, we only considered the natural broadening due to the semiconductor's intraband relaxation process, the non-natural broadening was omitted in respect that we had supposed no drilling holes in the gain materials beneath the waveguide and a negligible non-natural broadening due to the defect combination.

The simulation model is shown in Fig. 1. A triangular lattice PC with a line defect waveguide along ΓK direction is formed on an InP/InGaAsP/InP heterostructure with a layer of InGaAsP-MQW, whose emission wave length is 1.55 μm. Here, W and a denote the waveguide width and the lattice period, respectively. The air filling factor is kept at 33% and the holes are etched deep into the InP substrate. In this structure, the active layer of the device could be pumped by current or "internal light source" (ILS) technique [12]. The pumped area will be focused on the waveguides so that there will be no drilling holes in the gain area. This is helpful to the hypothesis that we could neglect the effect of the non-natural broadening on gain spectra due to the defect combination.

Gain improvement in PCWG attributes to its abnormal dispersion characteristics. First, we calculated the photonic energy band structure of W1 ($W = \sqrt{3}a$) and W3 PCWG ($W = 2\sqrt{3}a$) for TE polarization by plane wave expansion method (PWM) in 2-D with the effective index of 3.21 for the planar confinement in the vertical direction of the heterostructure. Figs. 2(a) and 3(a) show the photonic energy bands for the W1 and W3 PCWG, and the sketch maps of W1 and W3 PCWG were plotted in Figs. 2(b) and 3(c), respectively. The period of PC, $a = 360$ nm for W1 PCWG and $a = 410$ nm for W3 PCWG, was selected to make their first defect mode's centre correspond to the emission wavelength of InGaAsP MQW (1.55 μm). In order to find the dispersion curve in the photonic energy band which is corresponding to the first line defect mode, the first mode's magnetic field patterns of W1 and W3 PCWG were also shown in Figs. 2(c) and 3(d). The group velocity of the first line defect mode could be derived from the dispersion curve accordingly.

It can be seen that the group velocity of the first line defect mode in W1 PCWG descends at the band edge and can result in an increase of gain eventually. While in the W3 PCWG, more

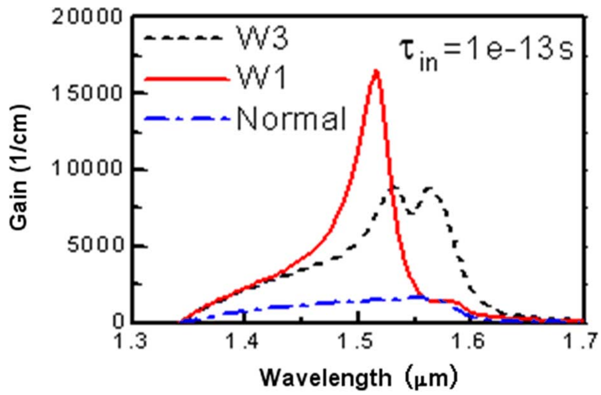

Fig. 4. Gain spectra of MQW with W1, W3 PCWG, and normal WG. The intraband relaxation time $\tau_{\rm in}$ used in our simulation is 10^{-13} s.

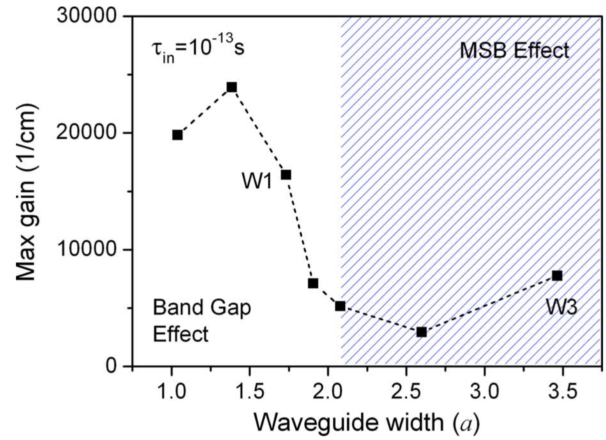

Fig. 5. Gain maximum of the first mode with different waveguide width PCWG structures. The intraband relaxation time $\tau_{\rm in}$ used in our simulation is 10^{-13} s. When W is smaller than $2.2a$, the gain enhancement is mainly caused by the low $v_{\rm g}$ of the first defect mode near the band edge. While, when W is larger than $2.2a$, the gain enhancement is mainly due to the low $v_{\rm g}$ of the first defect mode near the edges of MSB, which are shown in the shade region.

defect modes appear in its PBG, as well as a MSB appears in the dispersion curve of the first defect mode around $a/\lambda = 0.265$. The detail of the MSB was magnified in Fig. 3(b). In this case, the group velocity of the first defect mode reduces near the edge of the MSB. Therefore, the gain maximum will be caused by the low group velocity near MSB edges rather than that near the band edge. The gain spectra of InGaAsP MQW with W1 and W3 PCWG calculated using (1) is shown in Fig. 4. For comparison, the gain spectra of a normal WG is also presented in Fig. 4. The simulation results show a remarkable enhancement in W1 PCWG at the band edge, while the gain spectra of the W3 PCWG appears two peaks corresponding to the MSB. It can be seen from Fig. 4 that the complex defect modes in W3 PCWG degrade not only the transmission performance, but also the gain characteristics.

The intraband relaxation time $\tau_{\rm in}$ used in our simulation is 10^{-13} s. This will result in a 13-nm broadening width, approximatively. However, the mini-gap of MSB for W3 with a period of 410 nm is about 15 nm. Namely, the effect of natural broadening will mitigate the gain singularities near the band edge effectively. It will be another important reason for the nonzero gain in the mini-gap of MSB, besides internal loss [4].

By changing W from $0.6\sqrt{3}a$ to $2\sqrt{3}a$, the dependence of the first mode's gain maximum on the width of PCWG was calculated. Here, the lattice period a is different to make their first defect mode at the same wavelength of 1.55 μm. The corresponding gain peaks varying with different width of PCWG are plotted in Fig. 5. When W is smaller than $2.2a$, the gain enhancement is mainly caused by the low $v_{\rm g}$ of the first defect mode near the band edge. The gain maximum first increases and then decreases with widening W because that the change of the dispersion curve slope of first mode results in a changed $v_{\rm g}$, while, when W is larger than $2.2a$, the gain enhancement is mainly due to the low $v_{\rm g}$ of the first defect mode near the edges of MSB. Because the slope of the dispersion curves near the edges of MSB is not as moderate as that near the band gap edge, the gain maximum caused by MSB effect decreases in the shade region of Fig. 5. It is found that optimized W for the largest gain enhancement is around $1.4a$, which is still narrow for fabricating and realizing electrical injection.

B. Modified Mode Characteristics in 2-D PCWG With Microcavity Structure

We know PCWG with relative wide waveguide, such as W3 PCWG, is easy to be fabricated and to realize electrical injection. However, the gain performance of wide PCWG is worse than that of narrow PCWG because of the complex modes in the PBG, just as that stated above. Here, we propose a method to combine a microcavity structure inside the W3 PCWG to improve their mode characteristics, and further affect their gain performances.

First, the transmission spectra characteristics of the microcavities with different size and different "surrounding layer number," which is defined in Fig. 6(c), were simulated by 2-D FDTD. We used the perfectly matched layer (PML) as the boundary conditions and a Gaussian pulse as the launch source with the peak of 1.55 μm and pulse width of about 200 THz. The spatial width of the pulse is $2a$ in W3 PCWG. Here, a is the lattice period of the triangle PC. Other simulation parameters are set as followed: simulation domain size is $65a \times 9a$, the spatial grid size is $a/32$, the time step is $a/(32 \bullet {\rm c})$, where c is the light velocity in the vacuum, and FDTD stop time is 2^{17} time steps. We selected four different microcavity structures with increasing sizes of $3.90a^2$, $6.70a^2$, $10.39a^2$, and $17.32a^2$ for the simulation [shown in Fig. 6(b)], where the layer number changed from 1.5 to 3, as shown in Fig. 6(c). Fig. 6(a) shows the simulation results. It can be seen that for the frequency region of PBG, no transmission peak exits when the surrounding layer number is larger than 3, while the transmission spectra become continuous when the surrounding layer number is less than 1.5 where the layers is too few to filter the modes in W3 PCWG. On the other hand, the number of transmission peaks depends on the size of microcavity. By selecting appropriate size of $3.90a^2$ (one point defect structure) with the optimum surrounding layer number of 2.5, a single transmission peak can be obtained, which will benefit modifying mode characteristics in W3 PCWG. To analyze the modified mode characteristics of

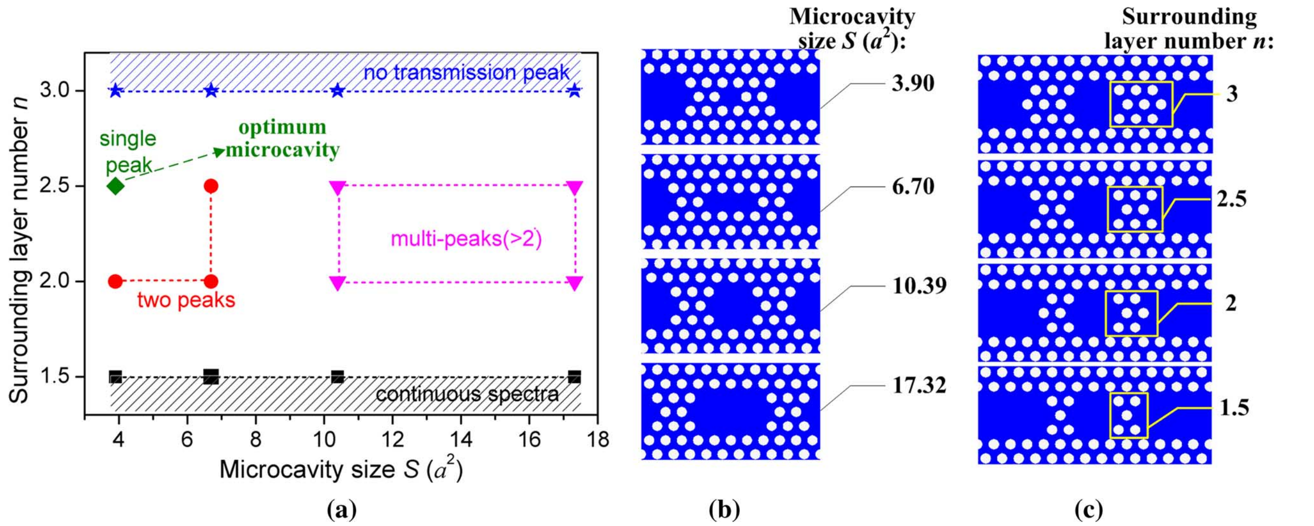

Fig. 6. (a) Dependence of transmission spectra characteristics in the PBG on different microcavity sizes S and surrounding layer numbers n. (b) Microcavity structures for different microcavity size S. (c) Definition of microcavity surrounding layer number n.

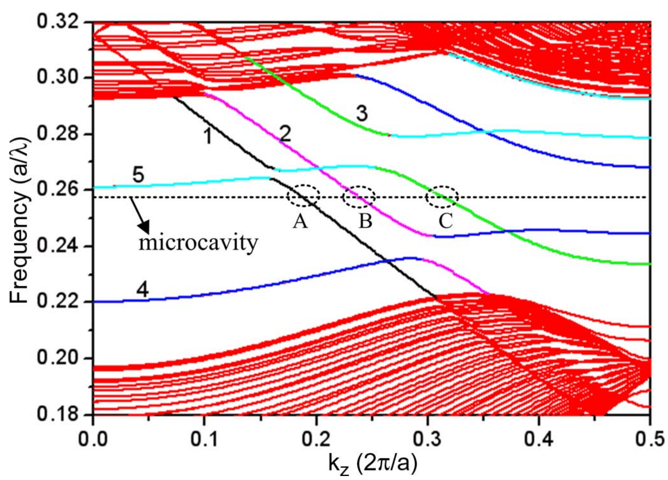

Fig. 7. Photonic energy band structures of W3 PCWG and defect frequency of the one point defect microcavity (blue dash line). Different defect modes in PBG of W3 PCWG are shown in different colors.

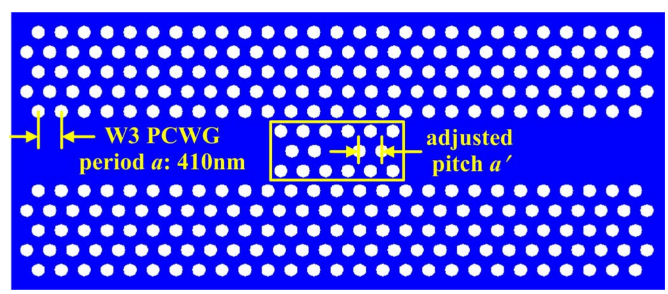

Fig. 8. Structure of W3 PCWG with the one point defect microcavity. W3 PCWG period a is 410 nm. The pitch of holes a' surrounding the microcavity in the yellow quadrate frame was adjusted.

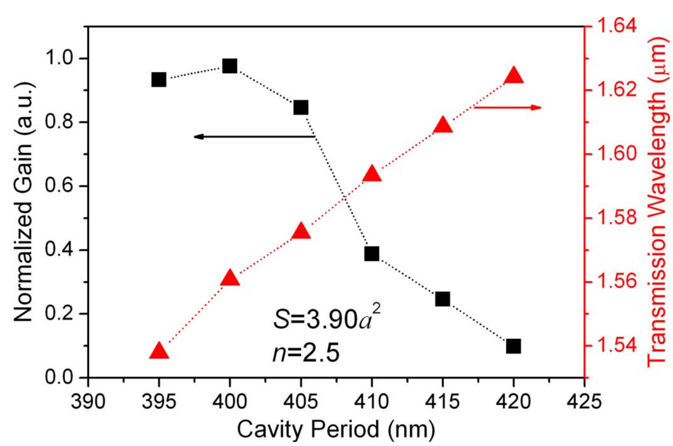

Fig. 9. Wavelength and gain of the transmission peak with different pitch of holes a' surrounding the microcavity, where the size S and layer number n of the one point defect microcavity are $3.90a^2$ and 2.5 layers, respectively.

the optimum one point defect microcavity, simulation results of photonic energy band structures with the defect frequency of this microcavity were shown in Fig. 7. Different defect modes in PBG of W3 PCWG were shown in different colors. Since the defect frequency of microcavity is very narrow, it was plotted as a line in the W3 PBG. Because the microcavity provides an additional selecting frequency mechanism, defect modes in W3 PCWG can be limited in the very narrow frequency range. Thus, the resonant modes between PCWG and microcavity in the photonic energy band graph will be several points A, B, C, as shown in Fig. 7. Among them, the mode with the lowest group velocity will have the largest gain [4]. Therefore, it is possible to select one longitudinal mode in W3 PCWG as a resonant frequency between the PCWG and the microcavity.

To have better gain characteristics, the pitch of holes surrounding the microcavity was adjusted to fit the defect frequency of microcavity to that where the first mode in W3 PCWG has the lowest group velocity. The adjusted structure is shown in Fig. 8. The wavelength and gain of the transmission peak with different pitch a' is shown in Fig. 9. When pitch a' is adjusted to 400 nm, the transmission peak wavelength is near the MSB edge where the first mode has the lowest group velocity. The transmission spectra of W3 PCWG with adjusted microcavity ($a' = 400$ nm) is shown in Fig. 10. It can be seen from Fig. 10 that without the microcavity, the transmitted

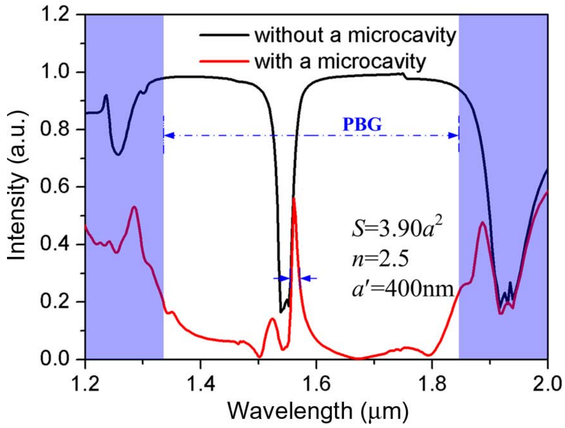

Fig. 10. Transmission spectra of W3 PCWG with and without a microcavity. The microcavity structure is shown in Fig. 8, and the pitch of holes a′ surrounding the microcavity is 400 nm.

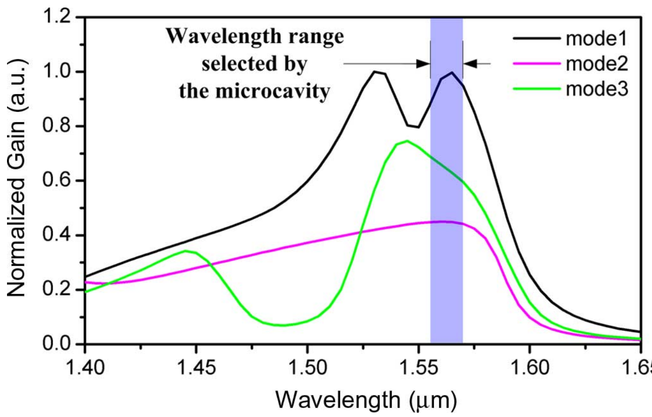

Fig. 11. Gain spectra of the first three modes in W3 PCWG. The transmitted wavelength range selected by the microcavity is shown in the shade region.

frequency range of W3 PCWG spread to the whole PBG with a dip around wavelength of 1.55 μm caused by the MSB effect, while the transmitted frequency range was significantly reduced by introducing the microcavity in PCWG. The resonant normalized frequency between the PCWG and the microcavity is just at the MSB edge. The gain spectra for the first three defect modes in W3 PCWG are calculated and shown in Fig. 11. It can be seen that the first defect mode has the largest gain among the three modes. Considering the transmission frequency selecting mechanism provided by the microcavity, the gain spectra can be limited in a narrow range. The transmitted wavelength range was shown in the shade region in Fig. 11. The reduction of the transmission range will weaken the longitudinal mode competition at the points with low group velocity. Therefore, we could get good lasing performance of the first mode with broad waveguide width.

III. Conclusion

We simulated gain spectra near the PCWG band gap edge by synthesizing the effect of group velocity and natural broadening. It was demonstrated that the gain in PCWG is influenced not only by the reduction of the group velocity, but also by the natural broadening due to the semiconductor's intraband relaxation process. The gain spectra of the first mode in different PCWG were analyzed by considering the intraband relaxation time τ_{in}. Based on this simulation results, we optimize the mode characteristics in W3 PCWG which has advantages of practical fabrication and electrical injection in active devices by combining a microcavity structure. Improved longitudinal mode characteristics can be obtained even with large waveguide width, such as W3 PCWG. This will benefit to design flexibility and fabrication tolerances.

Acknowledgment

The authors would like to thank Ms. H. Zhao for her valuable discussions and helpful comments.

References

[1] M. Notomi, A. Shinya, S. Mitsugi, E. Kuramochi, and H. Y. Ryu, "Waveguides, resonators and their coupled elements in photonic crystal slabs," *Opt. Exp.*, vol. 12, pp. 1551–1561, Apr. 2004.

[2] Y. Akahane, T. Asano, B. S. Song, and S. Noda, "High-Q photonic nanocavity in a two-dimensional photonic crystal," *Nature*, vol. 425, pp. 944–947, Oct. 2003.

[3] E. Schwoob, H. Benisty, C. Weisbuch, C. Cuisin, E. Derouin, O. Drisse, G. H. Duan, L. Legouezigou, O. Legouezigou, and F. Pommereau, "Enhanced gain measurement at mode singularities in InP-based photonic crystal waveguides," *Opt. Exp.*, vol. 12, pp. 1569–1574, Apr. 2004.

[4] J. P. Dowling, M. Scalora, M. J. Bloemer, and C. M. Bowden, "The photonic band edge laser: A new approach to gain enhancement," *J. Appl. Phys.*, vol. 75, pp. 1896–1899, Feb. 1994.

[5] S. Nojima, "Optical-gain enhancement in two-dimensional active photonic crystals," *J. Appl. Phys.*, vol. 90, pp. 545–551, Jul. 2001.

[6] H. Benisty, A. David, L. Martinelli, E. Viasnoff-Schwoob, C. Weisbuch, G.-H. Duan, K. Janiak, and H. Heidrich, "From modal control to spontaneous emission and gain in photonic crystal waveguides," *Photon. Nanostruct., Fundam. Appl.*, vol. 4, pp. 1–11, Feb. 2006.

[7] I. El-Kady, W. W. Chow, and J. G. Fleming, "Emission from an active photonic crystal," *Phys. Rev. B*, vol. 72, pp. 195110–195114, Nov. 2005.

[8] S. Olivier, M. Rattier, H. Benisty, C. Weisbuch, C. J. Smith, R. R. De, T. F. Krauss, U. Oesterle, and R. Houdre, "Mini-stopbands of a one-dimensional system: The channel waveguide in a two-dimensional photonic crystal," *Phys. Rev. B*, vol. 63, pp. 113311–113314, Mar. 2001.

[9] N. Susa, "Threshold gain and gain-enhancement due to distribute- feedback in two-dimensional photonic-crystal lasers," *J. Appl. Phys.*, vol. 89, pp. 815–823, Jan. 2001.

[10] P. S. Zory, *Quantum Well Lasers*. New York: Academic, 1993, ch. 1.

[11] J. M. Luttinger and W. Kohn, "Motion of electrons and holes in perturbed periodic fields," *Phys. Rev.*, vol. 97, pp. 869–883, Feb. 1955.

[12] R. Ferrini, D. Leuenberger, M. Mulot, M. Qiu, J. Moosburger, M. Kamp, A. Forchel, S. Anand, and R. Houdre, "Optical study of two-dimensional InP-based photonic crystals by internal light source technique," *IEEE J. Quant. Electron.*, vol. 38, no. 7, pp. 786–799, Jul. 2002.

[13] M. Asada, A. Kameyama, and Y. Suematsu, "Gain and intervalence band absorption in quantum-well lasers," *IEEE J. Quant. Electron.*, vol. 20, no. 7, pp. 745–753, Jul. 1984.

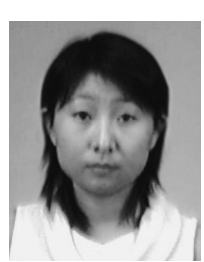

Kaiyu Cui was born in Jilin Province, China, on April 11, 1982. She received the B.S. degree in electronic engineering from Jilin University, Changchun, China, in 2005. Currently, she pursuing the Ph.D. degree in electrical engineering of Tsinghua University, Beijing, China.

Her current research interest is in the area of 2-D active photonic crystal devices.

Yidong Huang (M'97) received the B.S. and Ph.D. degrees in optoelectronics from Tsinghua University, Beijing, China, in 1988 and 1994, respectively.

From 1991 to 1993, she was with Arai Laboratories, Tokyo Institute of Technology, Japan, on leave from the Tsinghua University. She was with the Photonic and Wireless Devices Research Laboratories, NEC Corporation, from 1994 to 2003, where she was engaged in the research on semiconductor laser diodes for optical-fiber communication. In 2003, she joined the Department of Electronics Engineering, Tsinghua University, as a Professor. She is presently engaged in research on nanostructure optoelectronics.

Wei Zhang received the B.S. and Ph.D. degrees from the Department of Electronic Engineering, Tsinghua University, Beijing, China, in 1998 and 2003, respectively.

In 2003, he joined the Department of Electronics Engineering, Tsinghua University, where he is currently an Associate Professor. His major research interests include active and passive fiber devices and microstructure optoelectrical materials, especially microstructure fibers and their applications.

Jiangde Peng graduated from Tsinghua University, Beijing, in 1964.

He is currently a Professor with the Department of Electronic Engineering, Tsinghua University. He was a Senior Visiting Scholar with CNRS Laboratoire de Photophysique Moleculare, Universite d'Orsay, France (1973–1975), and with the Department of Electrical Engineering Systems, University of Southern California, Los Angeles (1997–1998). He has been engaged in research on active and passive fiber devices for WDM optical fiber communications, with specific emphasis on fiber amplifiers and lasers. At present, his primary interests focus on slow light, entangled photon-pair sources, and sensors based on micronanostructure materials. He is the author or coauthor of over 100 papers, 12 patents, and the textbook *Fundamentals of Optoelectronic Technologies* (Tsinghua University Press, 1988).

Prof. Peng is a member of the Optical Society of China and SPIE. He received the National Invention Award in 1997.